International Pipeline Conference — Volume I
ASME 1998

IPC1998-2026

APPLICATION OF THE QUARTZ CRYSTAL MICROBALANCE TO CORROSION INVESTIGATION

Hejian Sun, John C. Donini* and Kirk H. Michaelian
CANMET Western Research Centre
One Oil Patch Drive
Devon, Alberta, Canada T9G 1A8
and
Sankara Papavinasam and R. Winston Revie
CANMET Materials Technology Laboratory
568 Booth Street
Ottawa, Ontario, Canada K1A 0G1
* Deceased

ABSTRACT

The quartz crystal microbalance (QCM) provides an extremely sensitive technique for detecting small changes in mass and viscosity on the quartz crystal surface. QCM can be used in oil, gas or water without the problems of high solution resistance.

In order to use QCM to model pipeline corrosion, an iron quartz crystal electrode was prepared using an electrodeposition method. The reproducibility, effectiveness and accuracy of the iron QCM were tested in salt solution. The adsorption of amines was studied to investigate their effects on the corrosion behaviour of the iron QCM.

Key words: Corrosion, Inhibitor, Inhibitor film, Quartz Crystal Microbalance(QCM), Pipeline

Nomenclature:
A–the piezoelectrically active area
ΔF–the measured resonant frequency change
f_0–the resonant frequency of the quartz crystal prior to a deposition of a film
t_Q–the resonator thickness
μ_Q–the shear modulus of the AT-cut quartz
v_{tr}–the transverse velocity of sound in AT-cut quartz
ρ_Q–the density of quartz

1 INTRODUCTION

Quartz Crystal Microbalance (QCM) provides a new technique for the examination of electrode processes and electrode interface phenomena. Since Sauerbrey first recognized in the 1950's that these devices could be used to measure mass changes at the crystal surface[1], they have found wide application. Konash and Bastiaans[2] and Nomura[3] demonstrated the use of QCM in a liquid environment for the determination of mass change at the crystal surface. The use of the QCM in an electrochemical system to monitor mass changes at electrodes was first demonstrated by Jones and Meiure[4,5]. Nomura and co-workers first applied QCM in situ to determine copper and silver by electrodeposition[6,7]. In situ application of QCM to electrochemical systems was distinguished from nonelectrochemical applications such as the Electrochemical Quartz Crystal Microbalance (EQCM)[8]. EQCM has emerged as a powerful technique for detecting very small mass changes that accompany electrochemical processes at the electrode. Buttry and Ward have reviewed the applications of QCM and EQCM to investigate thin films, e.g. electrodeposition of metals, dissolution of metal films, electrovalency measurements of anion adsorption, hydrogen absorption in metal films, bubble formation, etc.[9] EQCM has been used to study redox and conducting polymer films[10] by Kaufman et al. Seo, Yoshida and Noda demonstrated the study of corrosion of iron thin film in aqueous solution[11]. Forslund and Leygraf developed a quartz microbalance sensor to monitor in situ atmospheric corrosion[12]. An application of QCM to localized corrosion has been demonstrated by Oltra and Efimov[13]. Pickering and co-workers used QCM to study the behaviour of triazole-iodide inhibitor[14].

The purpose of this research is to explore the possibility of using QCM to model pipeline corrosion in media of low conductivity, such as oil and oil containing a low percentage of water. The research will also provide a sound technique for investigating and predicting corrosion rates in the early stages of corrosion, and for assessing the deposition and removal of

inhibitor films. In this paper, the preparation of iron quartz crystals (IQC) by electrodeposition methods is presented, the properties of IQC are characterized, and the usefulness of IQC to investigate the film persistency of a batch inhibitor is illustrated.

2 EXPERIMENTAL

2.1 Experimental Method and Facilities

The QCM is, in principle, a piezoelectric device capable of sensitive mass measurements. The basic principle of QCM is that an oscillator circuit oscillates the quartz crystal at a frequency which is nearly equal to the resonant frequency. At the resonant frequency, the oscillation amplitude is a maximum[15]. The resonant frequency and the resonant admittance intensity are measured and displayed. The resonant frequency varies with the change in mass on the surface, and the resonant admittance intensity depends on the change of viscosity in solution[16].

The QCM can be used in gas, aqueous and oil phases without the problems of high solution resistance that pose difficulties when using electrochemical methods for measuring corrosion rates. The QCM determines changes in mass from the resonant frequency; therefore, the corrosion rates can be determined without knowledge of Tafel constants, which vary in the system.

The EQCM is actually the electrochemical version of the QCM, namely the QCM system combined with an electrochemical measuring system, e.g., a potentiostat/galvanostat. The EQCM system requires, in addition to conventional electrochemical equipment, an inexpensive frequency oscillator, a frequency counter, and commercially available AT-cut quartz crystal[17].

In this work, a quartz crystal analyzer made by EG&G is used. The system comprises the main unit, an oscillation circuit block, a quartz crystal holder and a quartz crystal. Figure 1 shows a schematic diagram of this QCM system.

The main unit consists of a frequency counter, ADC (Analog to Digital Converter), DAC (Digital to Analog Converter), a CPU (Central Processing Unit) and a display unit. The frequency counter measures the resonant frequency. The sample period can be either 0.1, 1.0 or 10.0 s. The shorter sample period yields a faster change in the resonant frequency becomes, but with a greater deviation in measured data. The resonant frequency and resonant admittance intensity are displayed in real time.

The oscillator circuit drives the quartz crystal and sends the frequency signal back to the main unit, where the signal is counted and displayed as the resonant frequency and resonant admittance intensity.

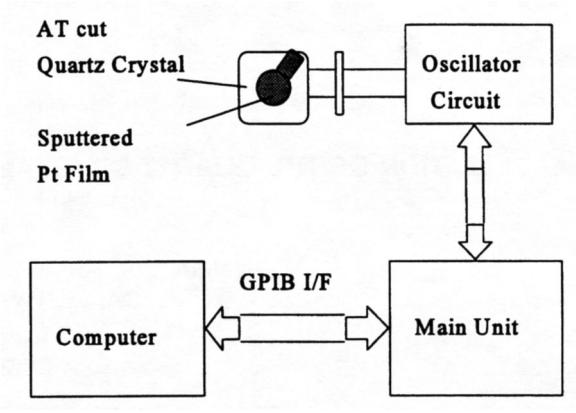

Fig. 1. Configuration of QCA917 System

The AT-cut quartz crystal is sandwiched between very thin (approx. 0.35 μm) round metal films. AT refers to the orientation of the crystal. This particular crystal was fabricated by cutting through a single crystal quartz rod at an angle of approximately 35° with respect to the crystallographic X axis.

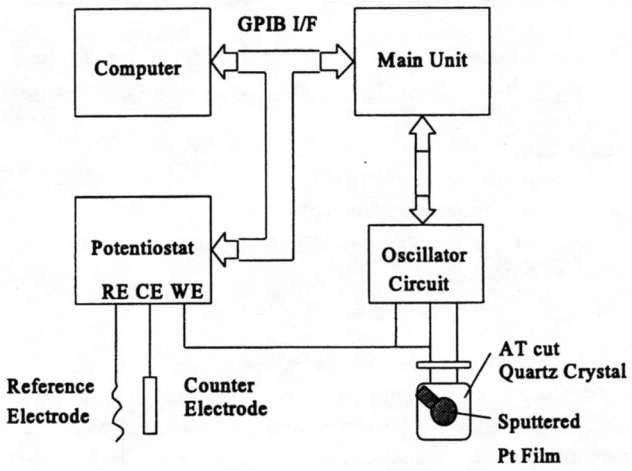

Fig. 2. Configuration of EQCM System

A typical configuration of the EQCM, in which a potentiostat has been introduced, is shown in Fig. 2. One side of the quartz crystal electrode, which is exposed to the solution, functions as a working electrode. The other side is isolated from the working electrode.

2.2 Preparation of Iron Quartz Crystal Electrode

A 9 MHZ, AT-cut quartz crystal was used in this work. It was coated on both sides by sputter deposition of titanium (thickness 50 nm) and platinum (thickness 300 nm). The coated area was 0.2 cm^2.

On one side, iron was electrodeposited using sulphate and fluoborate baths. The chemical composition and electroplating parameters are presented in Table 1. The electrodeposition was carried out galvanostatically in fluoborate and sulphate baths with current density 0.5 amp/dm^2 and 0.1 amp/dm^2, respectively.

Table1 Chemical Composition and Parameters for Electro-deposition of Iron

Chemicals	Fluoborate	Sulphate
$Fe(BF_4)_2$	223 mL/L	
$FeCl_2 \cdot 4H_2O$	311 g/L	
NH_4Cl	40.1 g/L	
Sodium Lauryl Sulphate	0.1g dissolved in hot water	
$FeSO_4 \cdot 7H_2O$		200 g/L
$MgSO_4 \cdot 7H_2O$		40 g/L
$NaHCO_3$		27 g/L
pH	3.3, adjusted with concentrated HCl	
Current density (amp/dm^2)	0.5	0.1
Temperature (°C)	60	25
Time (min.)	30	60
Thickness (μm)	2.5	1

2.3 Corrosion Test

The evaluation of the properties of an IQC has been carried out in the laboratory. Corrosion tests consisted of both galvanostatic and free exposure tests in deoxygenated neutral and low-pH 0.1 M sodium perchlorate solution (pH 2.0) at 25° and 50°.

2.4 Evaluation of Inhibitor Behaviour

The efficiency of an inhibitor depends largely on the structure and performance of the inhibitor film on the protected metal surface. In order to evaluate the inhibitor film persistency, an alkylamine with CH-chain length of 12 and a batch inhibitor have been studied in the laboratory. The amine, at a concentration of 1 mM, was added to a 0.1 M $NaClO_4$ solution deoxygenated with helium gas, which was adjusted to pH 2.0 by addition of 1 M HCl. The iron QCE was immersed in the solution, and the resonant frequency was recorded.

The resonant frequency of IQC in air was used as a basis for calculation of the amount of adsorbed inhibitor. The IQC was immersed in the inhibited solvent for one hour. The concentration of the batch inhibitor was 2000 ppm. After one hour, the iron QCE was removed from the solution and dried. Again the resonant frequency of the iron QCE was obtained in air. The weight of the adsorbed inhibitor on the surface of the QCM was calculated from the difference in frequency according to the calibration.

The iron QCE was again immersed in a deoxygenated 0.1 M $NaClO_4$ solution (pH 2.0) and the resonant frequency was recorded.

3 Results and Discussion

3.1 Properties of Deposited Iron

The change of resonant frequency during the electrodeposition of iron on the surface of the QCE was measured, and the results are presented in Fig. 3. Because the current was constant, the rate of mass change should theoretically be constant. The deposition rate in fluoborate is faster than in sulphate because of the higher current density in fluoborate bath. The relation between the mass change, Δm, and the change in the resonant frequency of the quartz crystal, ΔF, is described by the Sauerbrey equation[1]:

$$\Delta F = \frac{-2 f_0^2 \times \Delta m}{A\sqrt{\mu_Q \times \rho_Q}} \qquad (1)$$

where ΔF is the measured resonant frequency change, f_0 represents the frequency of the quartz crystal prior to film deposition, Δm is the mass change, A stands for the piezoelectrically active area, ρ_Q is the density of quartz, 2.648 g/cm^3, and μ_Q denotes the shear modulus of AT-cut quartz, 2.947 × 10^{11} dyne/cm^{-2}. The frequency of the acoustic wave fundamental mode is given by the equation,

$$f_0 = \frac{v_{tr}}{2\, t_Q} \qquad (2)$$

where v_{tr} is the transverse velocity of sound in AT-cut quartz, 3.34 × 10^4 m/s, and t_Q is the resonator thickness. Equation 2 shows that the relation between resonant frequency change and mass change is linear.

The amount of iron deposited during the same time under the same current density should be constant. The lines in Fig. 3 show the correlation to the theoretical analysis.

SEM photographs of iron film deposited from fluoborate and sulphate baths are shown in Fig. 4-7. The iron film deposited in fluoborate has a more uniform surface than in sulphate. In the following experiments, the iron quartz crystals were electrodeposited in fluoborate under the conditions presented in Table 1.

3.2 Corrosion Behaviour of the Iron QCM in Brine

Galvanostatic corrosion studies were carried out with a constant anodic current density of 10 $\mu A/cm^2$ at 25°C and 50°C using IQC as working electrode, Ag/AgCl as reference electrode and a 1 cm^2 platinum plate counter electrode. The electrolyte was 0.1 M $NaClO_4$ deoxygenated with helium gas. The results are shown in Fig. 8. The $NaClO_4$ test solution was selected to eliminate the effect of anions in solution on the mass change of the QCM, because ClO_4^- is a nonselective adsorbing anion.

In order to assess the adsorption effect of anions, the selectively adsorbed anion, SO_4^{2-}, was tested. The result is presented in Fig. 9, clearly indicating that anions cause an increase in the weight on the surface of QC electrode.

One of the important properties of the AT-cut quartz crystal is stable vibration performance with change of temperature. In Fig. 8, the temperature has obviously affected the QCM results. Further experiments on the effect of temperature on QCM performance have been carried out; the results are shown in Fig. 10.

The relationship between resonant frequency and temperature in the measured temperature range is linear. We can expect that the resonant frequency is a linear function of both mass change and temperature,

$$f = a\ m + b\ T + C \qquad (3)$$

The results obtained when an iron QCM was exposed to deoxygenated 0.1 M $NaClO_4$ of pH 2.0 at ambient temperature are presented in Fig. 11. The data indicate a very rapid weight loss, larger than that in the galvanostatic experiments with an anodic current density of 10 $\mu A/cm^2$.

3.3 Evaluation of Inhibitor Properties

Figure 12 shows the change of resonant frequency of an iron QCE during exposure to solvent with a batch inhibitor at a concentration of 2000 ppm. Frequency decreases with increasing time, indicating that the mass on the surface of iron QCE increases with time; in other words, inhibitor is being adsorbed on the surface. The difference in resonant frequency of the iron quartz crystal in air, before and after exposure to solution, is 394 Hz. From the calibration of the QCM system, its sensitivity is 1.1 nanogram/Hz, so that the increase of mass on the surface is 441 ng. Infrared spectroscopy confirmed the existence of nitrogen-containing chemicals on the surface after one hour of exposure of iron to solvent with 2000 ppm batch inhibitor.

The iron QCM coated with inhibitor film was introduced into the deoxygenated 0.1 M $NaClO_4$ solution of pH 2.0. During the exposure, the resonant frequency was recorded; the results are presented in Fig. 13. In this diagram there is a critical time before which the system has a very low corrosion rate because of inhibitor film persistence. After the critical time, the corrosion rate increases dramatically.

The effect of alkylamine on the corrosion rate of the IQC is presented in Fig. 14. The corrosion rate of iron QCE is slightly reduced by adding 1 mM dodecylamine to the solution.

4 CONCLUSIONS

- QCM is a powerful technique for detecting extremely small mass changes on the electrode surface, and can be used to detect corrosion at a very early stage.

- QCM can be used to study inhibition and inhibitor films. It will also be very useful to investigate adsorption and desorption processes on the surface of the electrode. It is very user friendly for evaluating inhibitor film persistency.

ACKNOWLEDGMENTS

The authors gratefully acknowledge the Federal Interdepartmental Program of Energy R & D (PERD) for financial support.

The authors appreciate all CANMET/WRC-MTL personnel for their helpful discussions and suggestions. The authors thank Randy Mikula, CANMET/WRC, for his kind help in SEM analysis.

REFERENCES

1. Sauerbrey, G., "The Use of Quartz Oscillators for Weighing Thin Layers and for Microweighing", Z. Phys. 155, 206 (1959).

2. Konash, P. L., and Bastiaans, G. J., "Piezoelectric Crystal as Detectors in Liquid Chromatograghy", Anal. Chem. 52, 1929(1980).

3. Nomura, T., "Single-Drop Method for determination of Cyanide in Solution with a Piezoelectric Quartz Crystal", Anal.

Chim. Acta 124, 81 (1981).

4. Jones, J. L., and Meiure, J. P., "A Piezoelectric Transducer for Determination of Metals at the Micromolar Level", Anal. Chem. 41, 484 (1969).

5. Meiure, J. P., and Jones, J. L., "Electrgravimetric Trace Analysis on a Piezoelectric Detector", Talanta 16, 149 (1969).

6. Nomura, T., Nagamune, T., Izutsu, K., and West, T. S., "New Electrolytic Method of Metal-Ion Analysis with a Piezoelectric Quartz Crystal and Its Application to the Determination of Minute Amounts of Copper (II)", Bunseki Kagaku 30, 494 (1981).

7. Nomura, T., and Iijima, M., "Electrolytic Determination of Nanomolar Concentration of Silver in Solution with a Piezoelectric Quartz Crystal", Anal. Chim. Acta 131,97 (1981).

8. Buttry, D. A., "Applications of the Quartz Crystal Microbalance to Electrochemistry", Electranalytical Chemistry, Vol. 17, edited by Allen J. Bard, Marcel Dekker, New York, Basel, Hong Kong, 1996, pp. 2-85.

9. Buttry, Daniel A., and Ward, Michael D., "Measurement of Interfacial Processes at Electrode Surfaces with the Electrochemical Quartz Crystal Microbalance", Chem. Rev., 92, 1355 (1992).

10. Kaufman, J.N., Kanazawa, K.K., and Street, G.B., "Gravimetric Electrochemical Voltage Spectroscopy: in situ Mass Measurements during Electrochemical Doping of the Conducting Polymer Polypyrrole", Phys. Rev. Lett., 53, 2461 (1984).

11. Seo, Masahiro, Yoshida, Kengo and Noda, Kazuhiko, "A Quartz Crystal Microbalance Study of the Corrosion of Iron Thin Films in Neutral Aqueous Solution", Materials Science and Engineering, A198, 197 (1995).

12. Forslund, M. and Leygraf, C., "A Quartz Microbalance Probe Developed for Outdoor in Situ Atmospheric Corrosivity Monitoring", Journal of The Electrochemical Society, 143(3), 839 (1996).

13. Oltra, R., and Efimov I.O., "Calibration of an Electrochemical Quartz Crystal Microbalance during Localized Corrosion", Journal of The Electrochemical Society, 141(7), 1838(1994).

14. Pickering, H.W., Weil, K.G. and Sakurai, T., "Quartz Crystal Microbalance and Scanning Tunneling Microscopy Studies of Triazole Inhibition of Copper", Proceedings of the 8th European Symposium on Corrosion Inhibitors (8SEIC), Vol.1, pp. 15, Ferrara, September, 1995.

15. Resnick, Robert and Halliday David, "Physics", Part I, John Wiley & Sons, Inc., New York, p.373 (1966).

16. "Quartz Crystal Analyzer Instruction Manual, Model QCA917", SEIKO EG&G, 1994.

17. Ward, M.D., "Principles and Applications of the Electrochemical Quartz Crystal Microbalance", Physical Electrochemistry: Principles, Methods, and Applications, edited by Israel Rubinstein, Marcel Dekker, New York, 1995, pp.293-338.

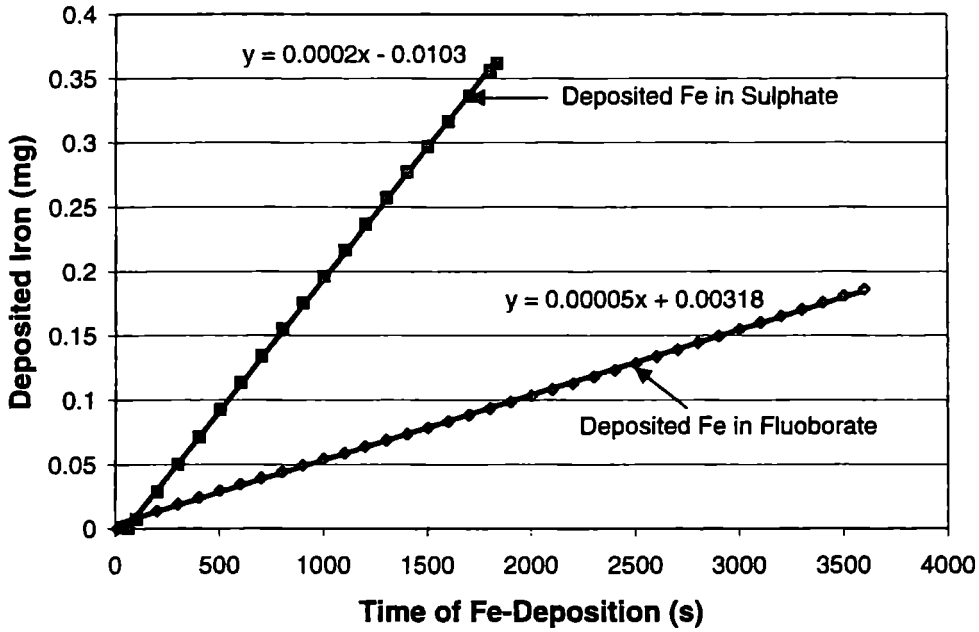

Fig.3 The Relationship between the Mass of Deposited Iron and the Deposition Time in Two Different Baths

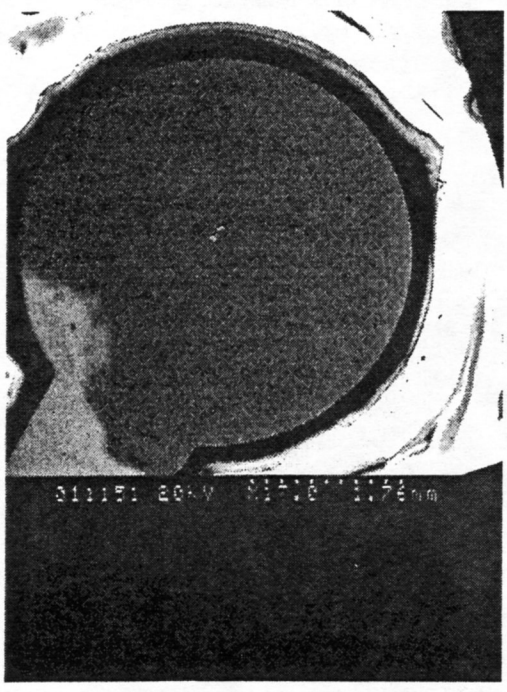

Fig. 4 SEM Surface Image of Deposited Iron in Sulphate Bath

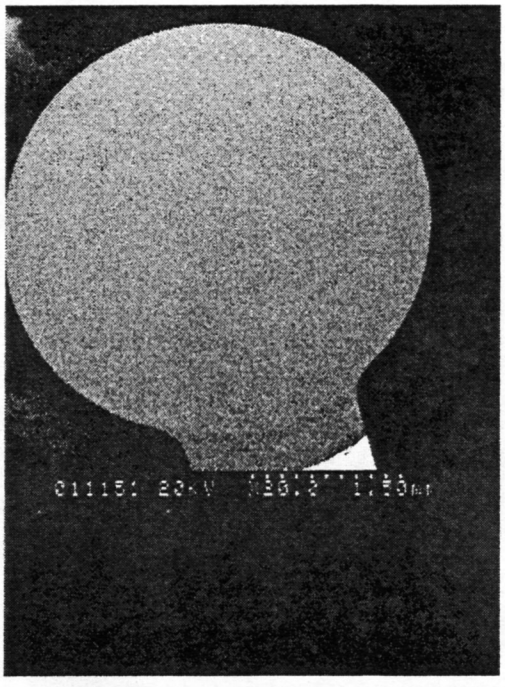

Fig. 5 SEM Surface Image of Deposited Iron In Fluoborate Bath

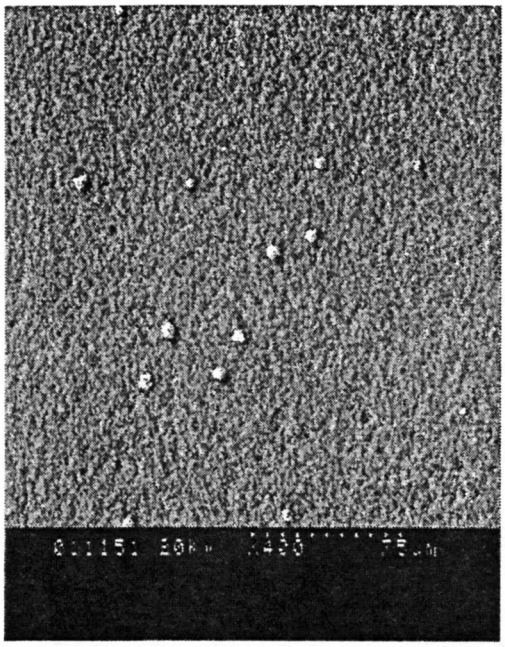

Fig. 6 SEM Surface Image of Deposited Iron in Sulphate Bath

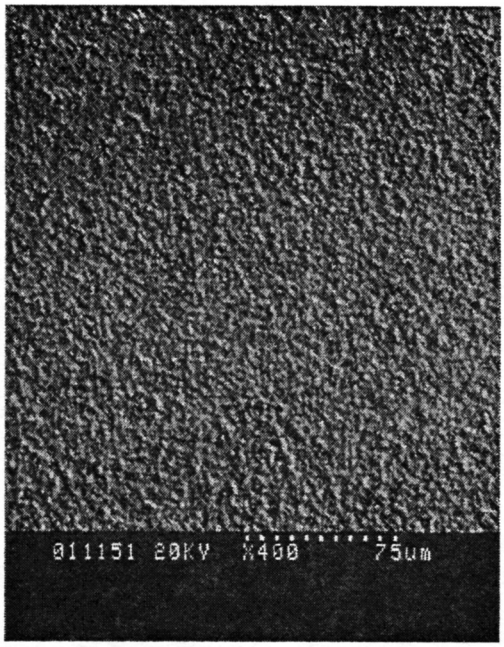

Fig. 7 SEM Surface Image of Deposited Iron In Fluoborate Bath

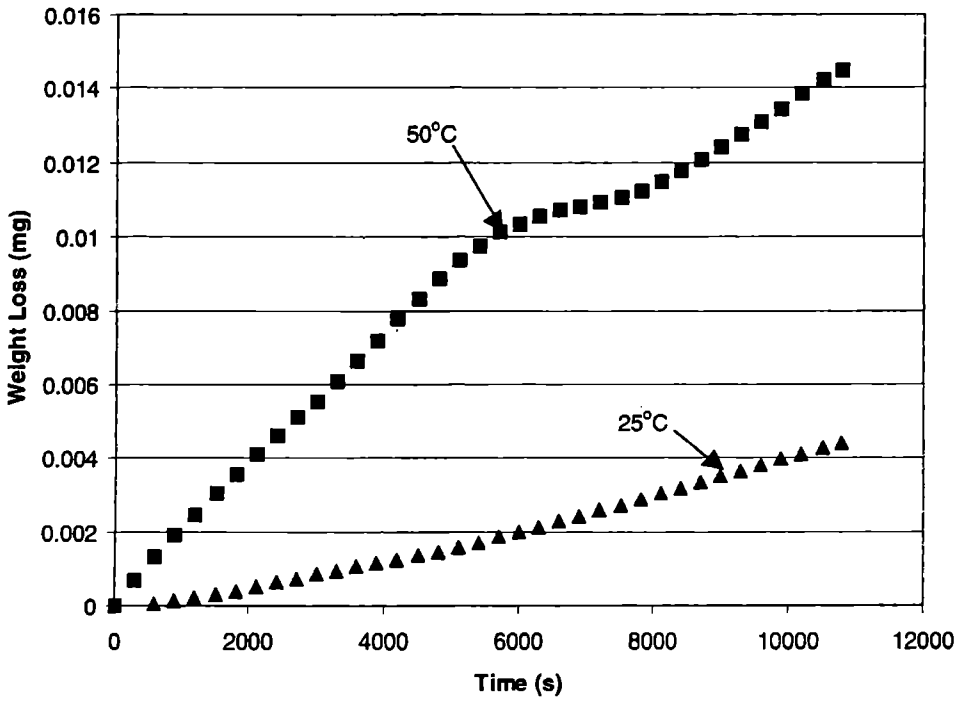

Fig. 8 The Effect of Temperature on the Corrosion Rate of IQC in 0.1 M $NaClO_4$ at 25° C and 50° C at an anodic current density of 10 $\mu A/cm^2$

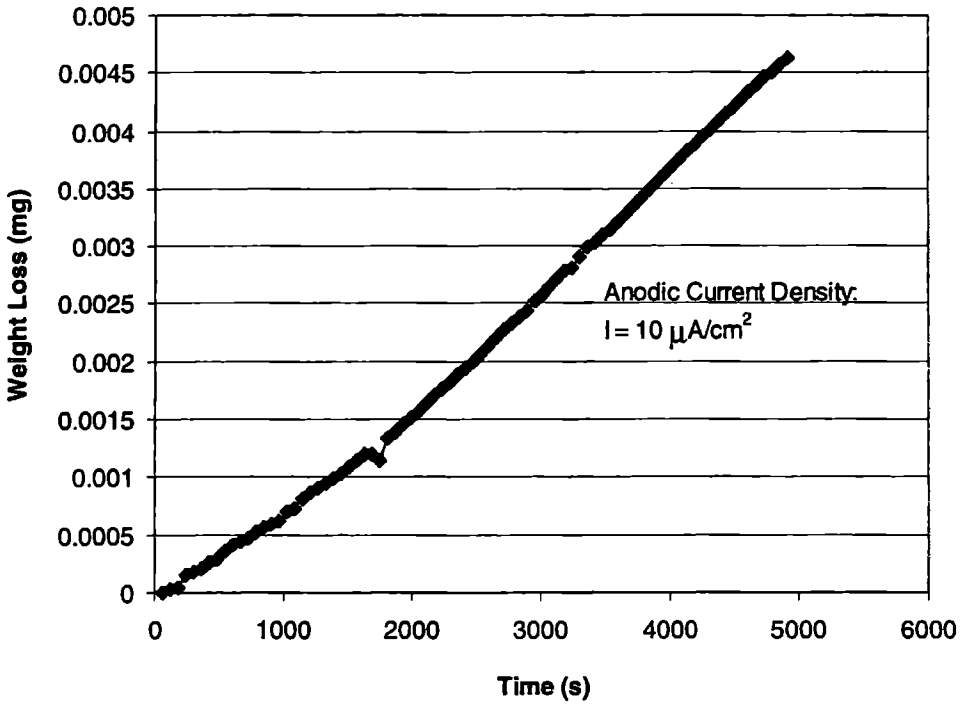

Fig. 9 Corrosion Test of the IQC in 0.1 M Na_2SO_4 at 25° C

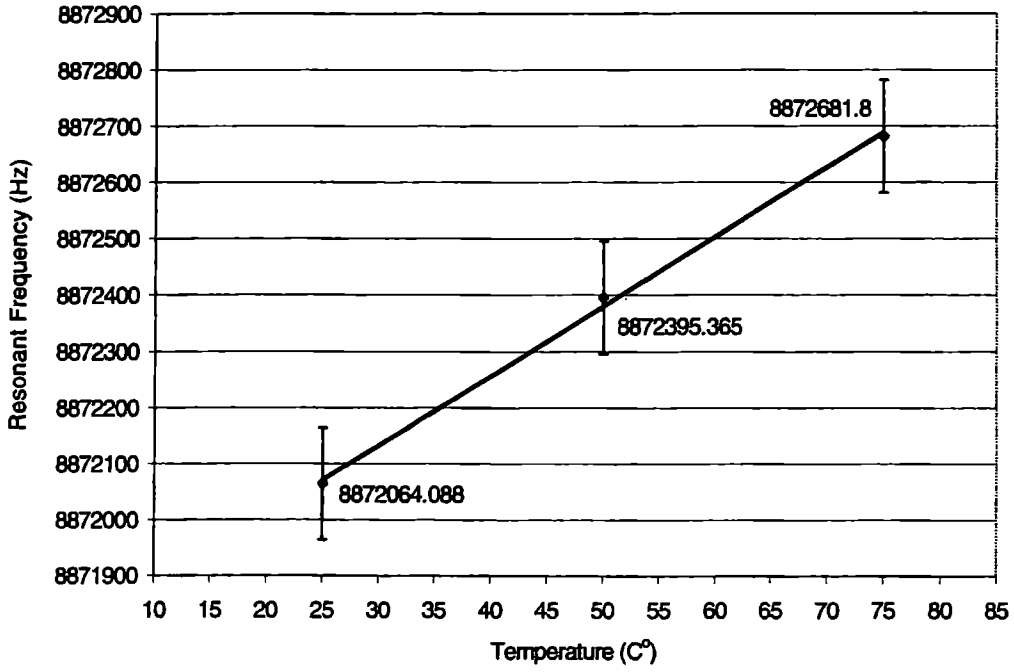

Fig. 10 Effect of Temperature on the Resonant Frequency of QCE in Deionized Water

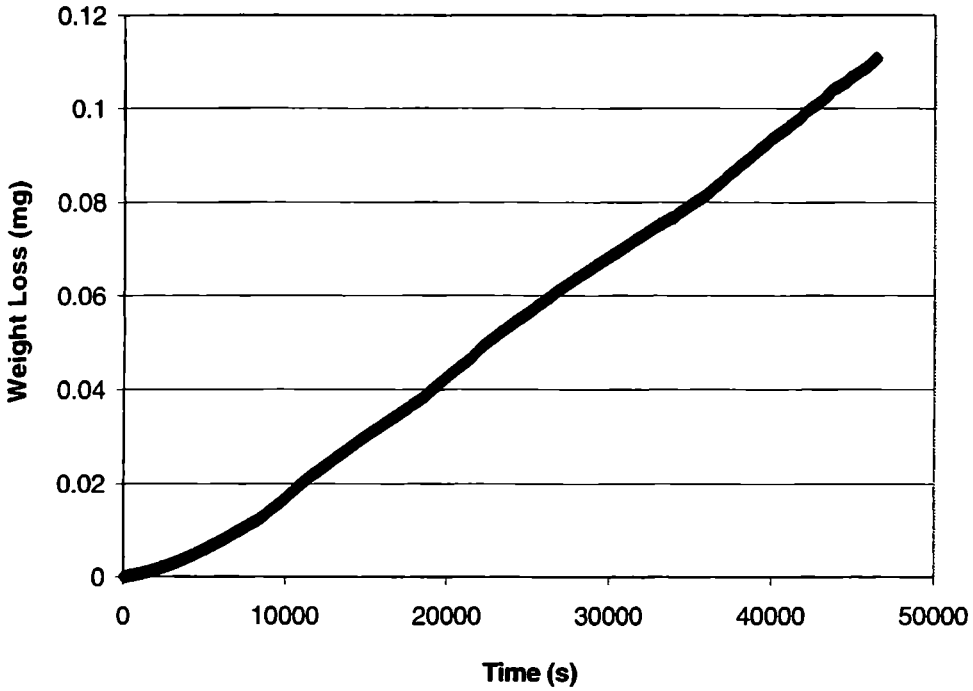

Fig. 11 Corrosion Test of Iron QCM in 0.1 M $NaClO_4$, pH 2.0

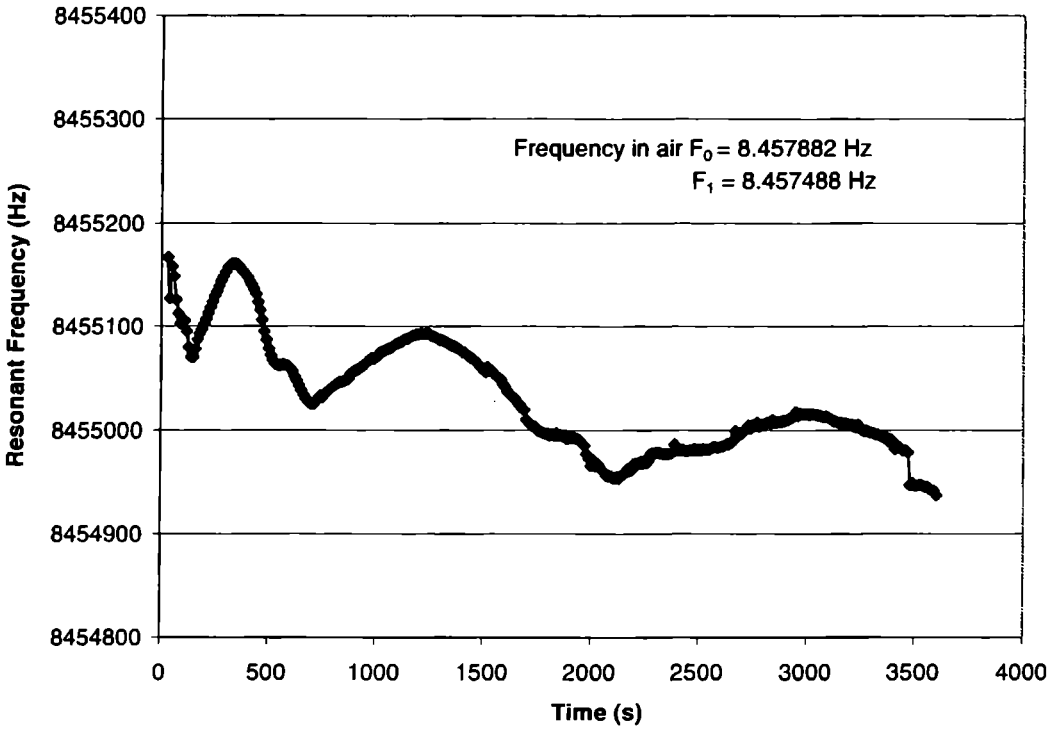

Fig. 12 Fe-QCE in Toluene with 2000 ppm Batch Inhibitor for 1 Hour

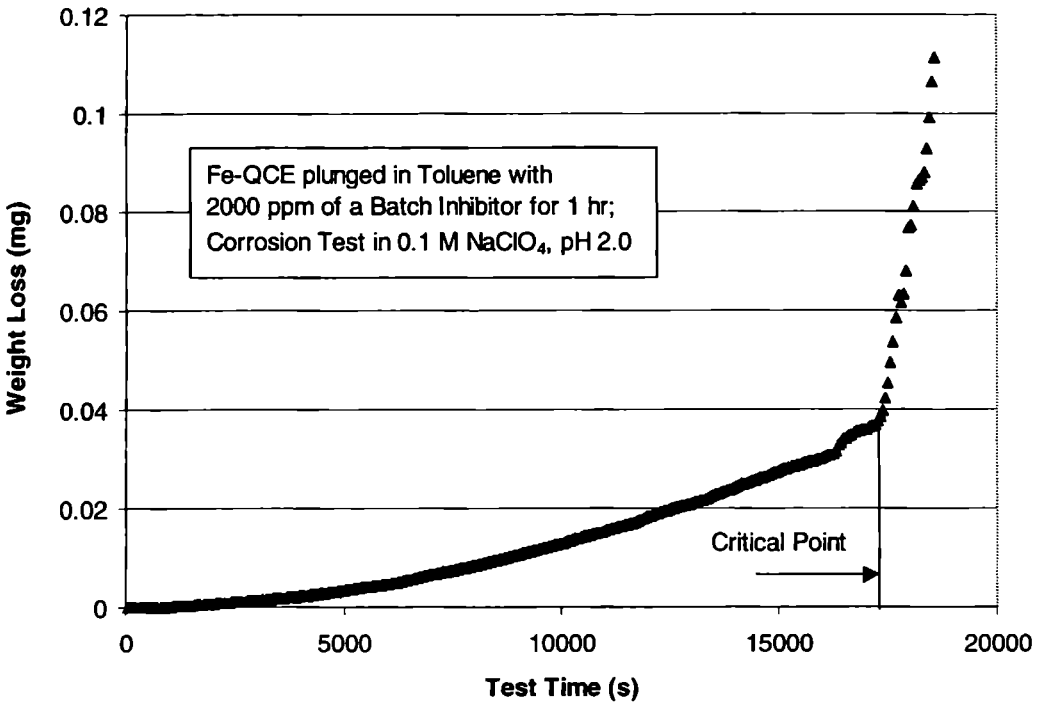

Fig. 13 Corrosion Behaviour of an Iron QC after treatment in a Batch Inhibitor, 25° C

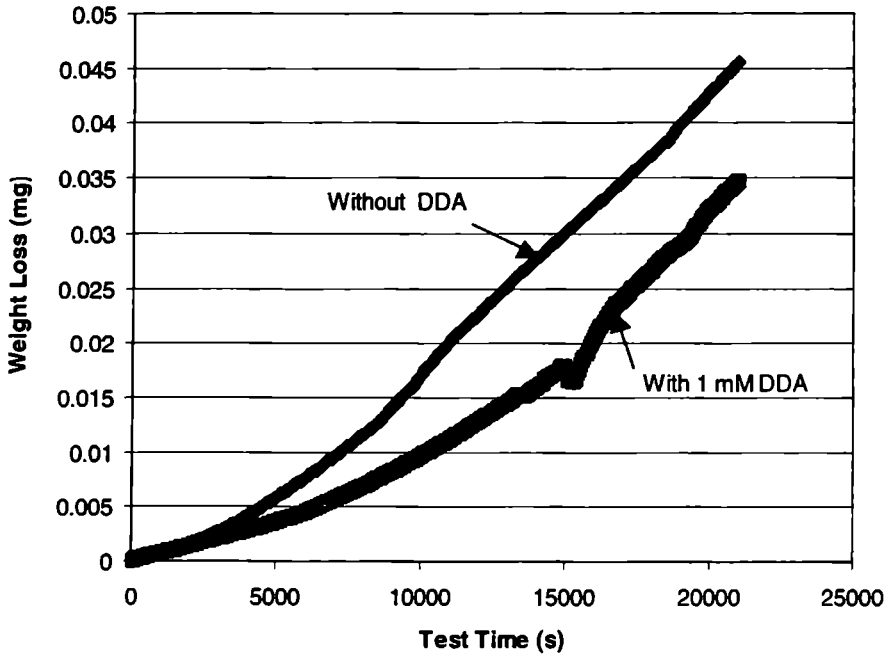

Fig. 14 Comparison of Corrosion Behaviour of Iron QCM in 0.1 M $NaClO_4$, pH 2.0, with and without Dodecylamine, 25° C